International Communications in Heat and Mass Transfer 86 (2017) 25–31

Contents lists available at ScienceDirect

International Communications in Heat and Mass Transfer

journal homepage: www.elsevier.com/locate/ichmt

Artificial neural network modeling of nanofluid flow in a microchannel heat sink using experimental data

Mohammad Mahdi Tafarroj[a], Omid Mahian[b,*], Alibakhsh Kasaeian[c], Kittipong Sakamatapan[d], Ahmet Selim Dalkilic[e], Somchai Wongwises[d,f,*]

[a] Department of Mechanical Engineering, Ferdowsi University of Mashhad, Mashhad, Iran
[b] Renewable Energies, Magnetism and Nanotechnology Lab., Faculty of Science, Ferdowsi University of Mashhad, Mashhad, Iran
[c] Faculty of New Science & Technologies, University of Tehran, Tehran, Iran
[d] Fluid Mechanics, Thermal Engineering and Multiphase Flow Research Lab. (FUTURE), Department of Mechanical Engineering, Faculty of Engineering, King Mongkut's University of Technology Thonburi, Bangmod, Bangkok 10140, Thailand
[e] Heat and Thermodynamics Division, Department of Mechanical Engineering, Yildiz Technical University, Yildiz, Besiktas, Istanbul 34349, Turkey
[f] The Academy of Science, The Royal Institute of Thailand, Sanam Suea Pa, Dusit, Bangkok 10300, Thailand

ARTICLE INFO

Keywords:
Microchannel
Nanofluids
Nusselt number
Artificial neural network

ABSTRACT

The present paper deals with the artificial neural network modeling (ANN) of heat transfer coefficient and Nusselt number in TiO_2/water nanofluid flow in a microchannel heat sink. The microchannel comprises of 40 channels; each channel has a length of 4 cm, a width of 500 μm, and a height of 800 μm. In the ANN modeling of heat transfer coefficient and Nusselt number 23 and 72 datasets have been used, respectively. The experimental Nusselt number has been calculated based on three different thermal conductivity models, four volume fractions of 0, 0.5, 1, and 2%, two values of Reynolds number i.e. 400 and 1200 and three different heating rates including 50.6, 60.7, and 69.1 W. Therefore, the inputs that are introduced to the neural network are volume fraction of nanoparticles, Reynolds number, heating rate, and model number while the output of network is the Nusselt number. It is elucidated that an appropriately trained network can act as a good alternative for costly and time-consuming experiments on the nanofluid flow in microchannels. The average relative errors in the prediction of Nusselt number and heat transfer coefficients were 0.3% and 0.2%, respectively.

1. Introduction

Over the last decade, numerous studies both experimentally and numerically have been performed to appraise the nanofluids properties and their role in efficiency enhancement of energy systems (For example, refer to Refs. [1–10]). One of the challenges for assessing the nanofluid effect on the performance of thermal systems is difficulties in nanofluid preparation and relatively high expenses of production. One solution to save the time and reducing the expenses of experiments may be the implementation of soft computing methods such as Artificial Neural Network (ANN) to predict the efficiency of nanofluid-based thermal systems. Here, a brief review of some previous studies on modeling of nanofluid properties and applications using ANN is presented.

In 2009, Santra et al. [11] modeled natural convection of a non-Newtonian nanofluid (Cu/water) in a cavity using both CFD and ANN. A resilient-propagation (RPROP) algorithm was used for training the neural network. It was concluded that ANN could be more helpful than CFD from the time-saving viewpoint. Hojjat et al. [12] measured thermal conductivity of three different non-Newtonian nanofluids containing γ-Al_2O_3, TiO_2 and CuO nanoparticles and used ANN for modeling the experimental data. The inputs of ANN were temperature, nanoparticle volume fraction, and thermal conductivity of nanoparticles.

Balcilar et al. [13] used three different ANN approaches including multi-layer perceptron (MLP), generalized regression neural network (GRNN) and radial basis function (RBF) to model the pool boiling of TiO_2/water nanofluids. They found that ANN methods are able to predict the heat transfer coefficient with errors less than ± 5%. Yousefi et al. [14] estimated the relative viscosity of different nanosuspensions composed of various nanoparticles (i.e. CuO, SiO_2, Al_2O_3, TiO_2) and base liquids (i.e. water, ethanol, a mixture of propylene glycol and water, and a mixture of ethylene glycol and water) by designing a diffusional neural network. The modeling results were fitted with experimental data well. Esfe et al. [15] studied experimentally the thermal conductivity of ethylene glycol based nanofluids containing

* Corresponding authors.
E-mail addresses: omid.mahian@gmail.com (O. Mahian), somchai.won@kmutt.ac.th (S. Wongwises).

http://dx.doi.org/10.1016/j.icheatmasstransfer.2017.05.020

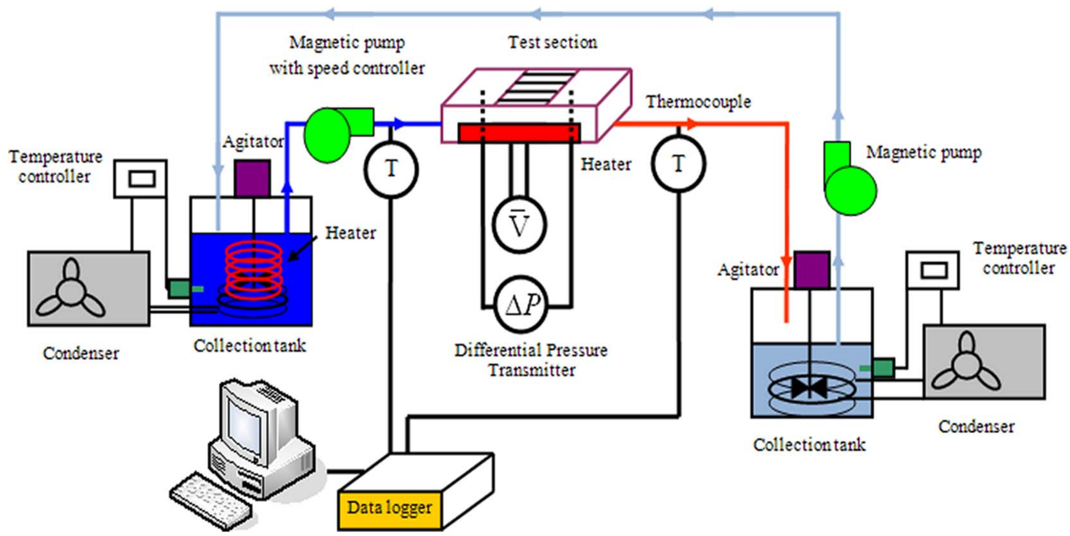

Fig. 1. Schematic of the experimental set-up [From Nitiapiruk et al. [30], with permission from Elsevier].

MgO particles with four different sizes including 20, 40, 50, and 60 nm where temperature changes between 25 and 55 °C, and concentration varies between 0 and 5%. Next, a neural network was trained to model the measured data of thermal conductivity by introducing volume fraction, nanoparticle dimension, and temperature as inputs of the network.

Bahiraei and Mashaei [16] first presented a three dimensional CFD model for Al_2O_3/water nanofluid flow in a canal with discrete heat sources and then using the simulation data they extended an artificial neural network to predict the heat transfer coefficient and pressure drop in the channel.

Esfe et al. [17] measured thermal conductivity of COOH-functionalized MWCNTs/water nanosuspensions and then implemented MLP technique to model the data. Temperature (between 25 and 55 °C) and nanofluid concentration (up to 1%) were the inputs of trained network. The results of modeling were in good agreement with experimental data.

Afrand et al. [18] used 48 experimental data obtained for viscosity of MWCNTs-SiO_2/AE40 nanolubricants to develop a correlation. Next, they designed an optimal ANN based on the derived correlation. The comparisons between outputs of the correlation and the optimized ANN revealed that the deviation margin of ANN results from experimental data is just 1.5% while the deviation margin reaches 4% in the case of correlation. Abdollahi and Shams [19] studied the nanofluid flow in a channel equipped to vortex generator numerically. They utilized neural network along with multi-objective genetic algorithm and CFD modeling to obtain the optimal nanofluid concentration, and position and shape of vortex generator in the channel. Ziaei-Rad et al. [20] solved numerically the nanofluid flow over a horizontal permeable stretching sheet under magnetohydrodynamic(MHD) flow by converting governing equations from partial differential to ordinary differential form. Effects of different parameters including suction/injection, nanofluid concentration, viscous dissipation and MHD parameter on the values of skin friction factor and Nusselt number have been evaluated. Next, using a multilayer neural network approach a model with excellent accuracy was presented to predict the Nusselt number and friction factor where the average difference between results of numerical solution and neural network model was less than 0.4%. Kalani et al. [21] used adaptive neuro fuzzy inference system (ANFIS) model and two different neural networks including RBF and MLP to predict the outlet temperature and electrical efficiency of a photovoltaic thermal (PVT) system using Zinc Oxide/water nanofluid. Particle Swarm Optimization (PSO) procedure was implemented to optimize the structure of the three models. It was found that ANFIS and RBF can estimate the desired outputs with a higher accuracy. To save the space, other related papers on modeling of nanofluid flow using the neural network are not reviewed here; as other instances, interested readers can refer to Refs. [22–28].

The above literature review reveals that most of the studies on neural network modeling of nanofluids have been conducted on thermophysical properties and not enough attention has been paid to use ANN for modeling of nanofluid flow in industrial thermal systems such as microchannel heat sinks. There is a conference paper released in 2008 that reports the application of ANN for modeling of Cu/water nanofluid flow in a microchannel heat sink. However, the modeling was done based on the results of an analytical analysis and not experimental data [29].

Based on the best knowledge of the authors, there is no study on neural network modeling of nanofluid flow in microchannel heat sinks using measured data, despite the high importance of microchannels in cooling of electronic devices. The present paper aims to extend a neural network to predict the Nusselt number and heat transfer coefficients due to nanofluid flow in a microchannel heat sink. The experimental data used in the present modeling have been extracted from our previous experimental work on the flow of TiO_2/water nanofluid in a microchannel heat sink composed of 40 channels [30]. It should be mentioned that the experiments on the microchannel heat sink were performed under real conditions in which domestic computers operate.

2. Experiments

A complete description of experimental set- up and procedure has been given in Ref. [30], but here a summary of the experimental study is represented. Fig. 1 depicts a schematic of the experimental set-up. The test section comprises of a microchannel heat sink with 40 channels and a heater in the bottom. Each channel has a length of 4 cm, a width of 500 μm, and a height of 800 μm. The heat was applied to the microchannel heat sink at three different rates including 50.6, 60.7, and 69.1 W. Water-based nanofluids containing TiO_2 nanoparticles at concentrations of 0.5, 1, and 2% have been prepared, and the results were compared with water. Experiments were performed under laminar regime of nanofluid flow. Nusselt number and heat transfer coefficients were estimated based on measured temperatures and heating rate. Nusselt number is related to heat transfer coefficients through thermal conductivity. For estimation of Nusselt number, three different thermal conductivity models have been used as follows:

Model 1: Maxwell equation is used to calculate thermal

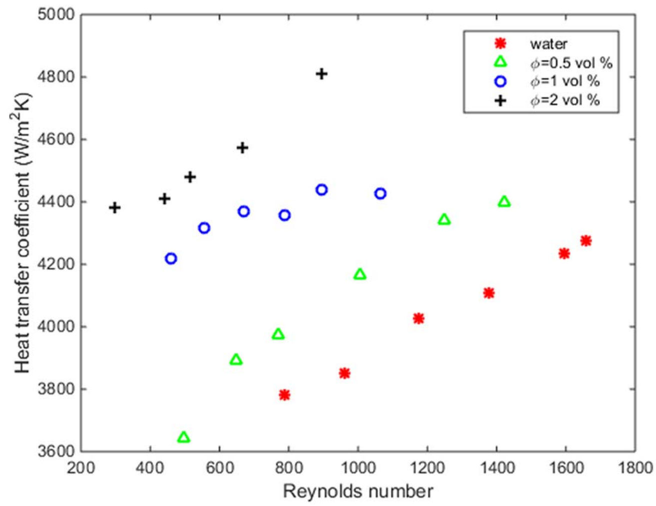

Fig. 2. Experimental heat transfer coefficient versus Reynolds number for heating rate of 69.1 W [30].

conductivity in model 1, it reads [31]:

$$\frac{k_{nf}}{k_f} = \frac{k_p + 2k_f + 2\phi(k_p - k_f)}{k_p + 2k_f - \phi(k_p - k_f)} \tag{1}$$

Model 2: Yu and Choi model is utilized to estimate the thermal conductivity in model 2 [32]:

$$\frac{k_{nf}}{k_f} = \frac{k_p + 2k_f + 2(k_p - k_f)(1+\beta)^3\phi}{k_p + 2k_f - (k_p - k_f)(1+\beta)^3\phi} \tag{2}$$

where $\beta = 0.1$.

Model 3: in this model, experimental data of Duangthongsuk and Wongwises [33] have been used:

$$\frac{k_{nf}}{k_f} = d + e\phi \tag{3}$$

where a, b, c, d and e are functions of temperature.

Fig. 2 has been presented as an instance of experimental results for

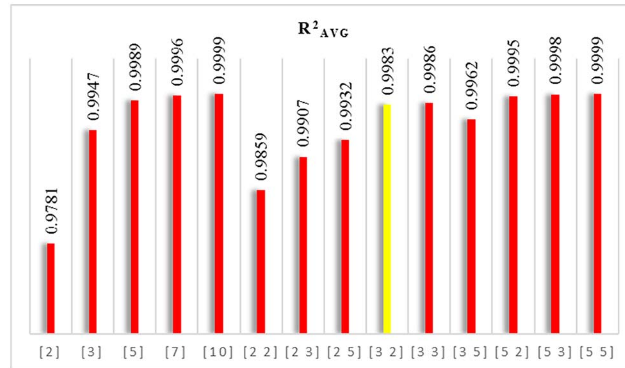

Fig. 4. Average of the correlation coefficients for the train data sets after 10 runs of each network structure to predict the heat transfer coefficients.

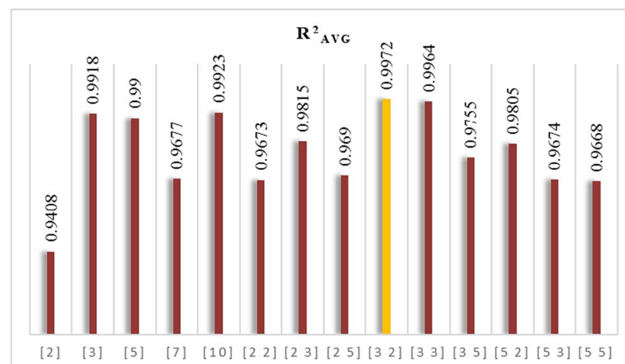

Fig. 5. Average of the correlation coefficients for the test data sets after 10 runs of each network structure to predict the heat transfer coefficients.

heat transfer coefficient in the microchannel heat sink. In this case, there are 23 data at volume fractions 0 to 2%, Reynolds numbers less than 1700 (laminar regime), and heating rate of 69.1 W. As shown, at a given nanofluid concentration, the heat transfer coefficient is an ascending function of Reynolds number. In addition, by loading of TiO_2 nanoparticles the heat transfer coefficient ameliorates. For example, at low Reynolds numbers (about 400), the heat transfer coefficient

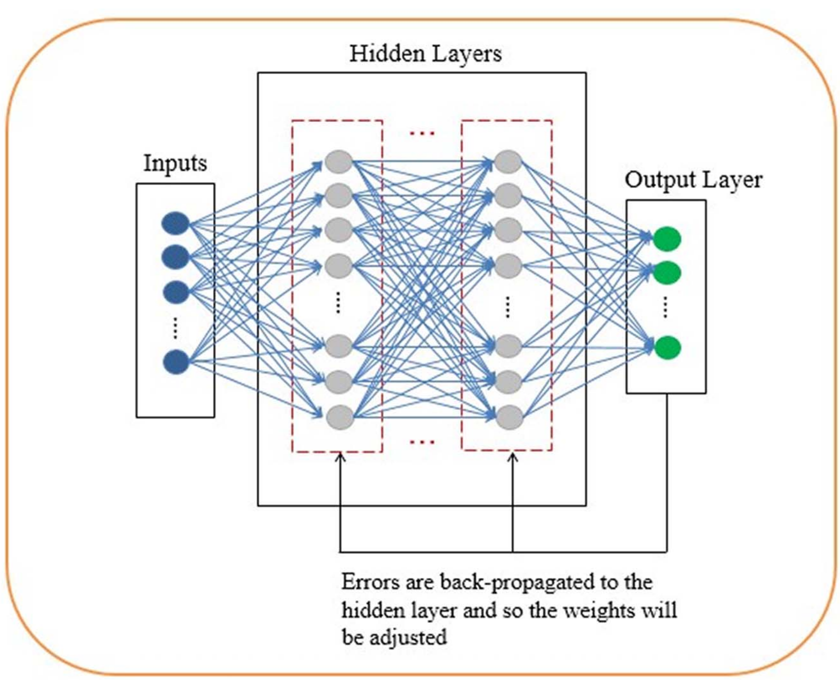

Fig. 3. The architecture of MLP network.

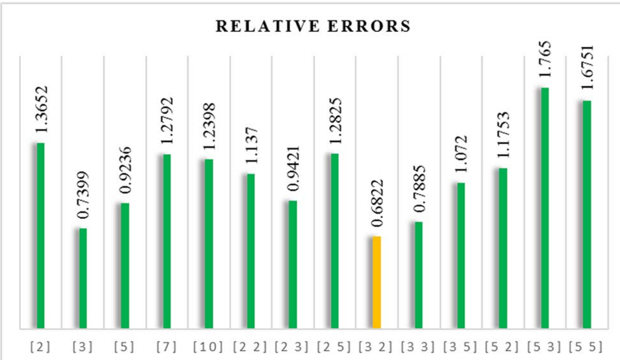

Fig. 6. Average of the relative errors for the test data sets after 10 runs of each network structure to predict the heat transfer coefficients.

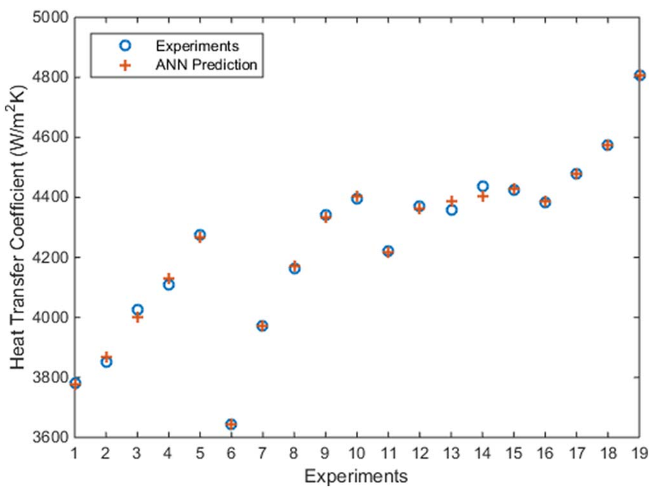

Fig. 7. The experimental results versus the network outputs for the train data set to predict the heat transfer coefficients.

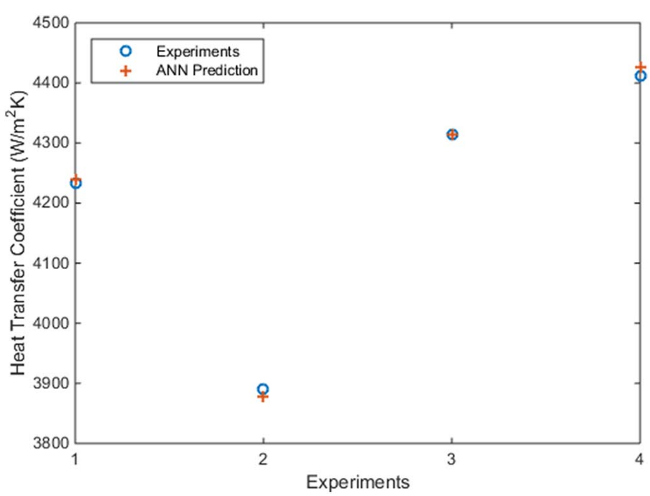

Fig. 8. The experimental results versus the network outputs for the test data set to predict the heat transfer coefficients.

enhances almost 5% with increasing the volume fraction from 1 to 2%. Brownian motion of nanoparticles and thermophoresis phenomenon may be the reasons behind the heat transfer enhancement in the microchannel.

3. Artificial neural network modeling

The inspiration behind the ANN is the brain. The human brain

Table 1
Comparison between the heat transfer coefficients predicted by ANN against the values obtained from experiments for the test data.

Experiment No.	Input 1 (*Re*)	Input 2 (Volume fraction (%))	Experimental Result (Heat transfer coefficient (W/m^{2}K))	Network Outputs (Heat transfer coefficient (W/m^{2}K))	Relative Error (%)
1	1594.87	0	4232.88	4222.59	0.1
2	649.304	0.5	3890.41	3897.14	0.3
3	554.485	1	4315.07	4314.60	0.04
4	440.395	2	4410.96	4440.20	0.3
					Average 0.2

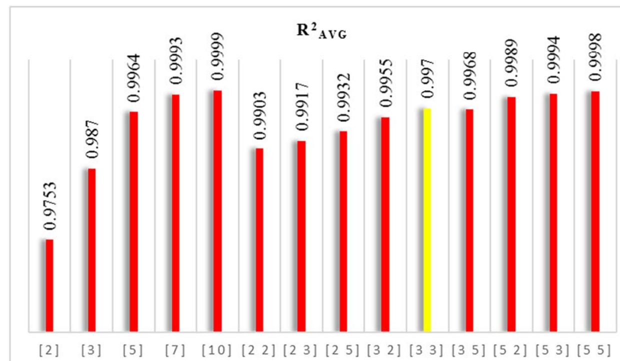

Fig. 9. Average of the correlation coefficients for the train data sets after 10 runs of each network structure to predict the Nusselt number.

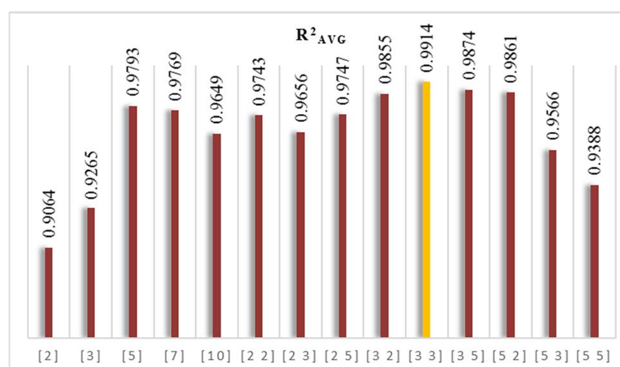

Fig. 10. Average of the correlation coefficients for the test data sets after 10 runs of each network structure to predict the Nusselt number.

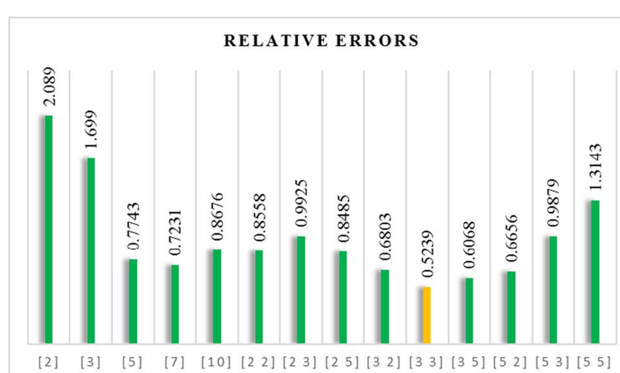

Fig. 11. Average of the relative errors for the test data sets after 10 runs of each network structure to predict the Nusselt number.

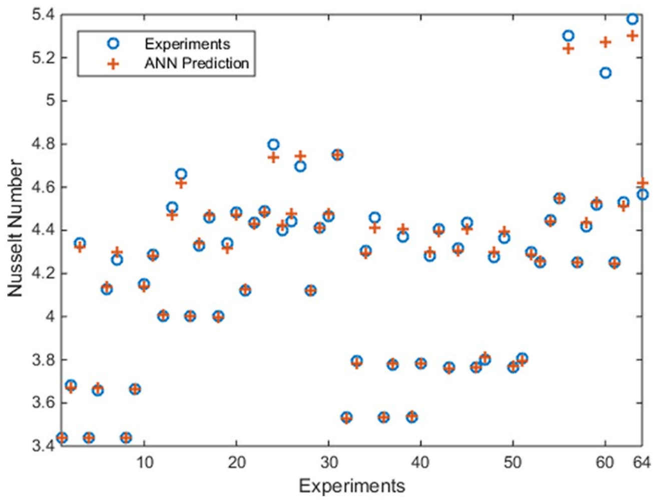

Fig. 12. The experimental results versus the network outputs for the train data set to predict the Nusselt number.

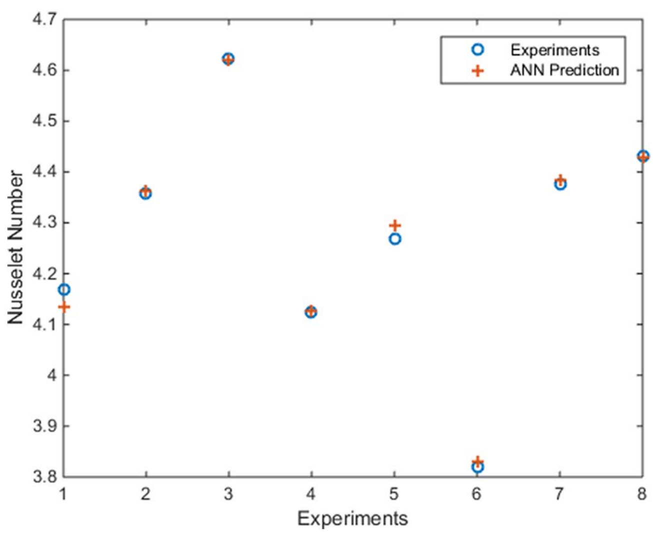

Fig. 13. The experimental results versus the network outputs for the test data set to predict the Nusselt number.

consists of a huge number of processing units connected just like a network. These units are named as "Brain Cells" or "Neurons". An ANN is trained to find a relationship between the inputs and outputs of a system. These networks are composed of some structural blocks called neurons just like the biological brain cells. These blocks are very simple computational units constructing the layers in which the relation between them determines the performance of the network. Neurons are arranged in such a structure that the output of every neuron in each layer is weighted and then acts as the input of the next layer. The number of hidden layers and also the number of neurons in each hidden layer can be determined after some trials and errors [34], but the number of inputs and outputs are imposed by the problem at hand. Each neuron in the hidden or output layers has an activation function also known as a transfer function. Neurons in output layer usually have a linear function like Eq. (4), but in hidden layers, some other functions are used like the hyperbolic tangent sigmoid transfer function which has been shown in Eq. (5). Using these activation functions, the outputs of the neurons are computed.

$$f(x) = x \tag{4}$$

$$f(x) = \frac{2}{1 + e^{-x}} - 1 \tag{5}$$

3.1. Error backpropagation learning (EBP) method

In the present study, a multi-layer perceptron (MLP) neural network has been implemented to model the relationships between the output and input variables. A simple representation of MLP network architecture has been shown in Fig. 3. In the learning phase, the output of the network is compared with the target value (results of experiments) and the computed error of the network is back-propagated to the hidden layers. Then, the weights will be adjusted by using these propagated errors. This learning method is called the error back-propagation (EBP) presented by Rumelhart and Mcclelland [35].

To explain how the EBP applied, for simplicity and without loss of generality, it has been assumed that the network has only one hidden layer. Each input is multiplied by weights of the hidden layer neurons (w_{ih}) and is added to a bias value, b_h, to form the activation a_h, this statement can be written in vector form as:

$$\mathbf{a} = \mathbf{W}^{\mathrm{T}}\mathbf{I} + \mathbf{B} \tag{6}$$

where **I** is the input vector, **W** is the weight matrix between inputs and hidden layer, **B** is the vector containing biases of hidden layer neurons, and **a** is a vector of each neuron activation.

After computing activations of all hidden neurons, outputs of all of them are estimated using the transfer function as:

$$o_h = \frac{2}{1 + e^{-a_h}} - 1 \tag{7}$$

where o_h is the output of hidden neuron number h. These latter calculated values will be weighted and summed to biases again to constitute the activations of the output layer, a_o. The linear transfer function is implemented and output, O, is computed. Then, the error is calculated as the difference between the computed outputs and their corresponding experimental results known as the target data. This procedure constructs the forward step of the backpropagation method and the estimated errors are back propagated through the network to adjust weights. Weights are adjusted using generalized delta rule as

$$w_{new} = w_{old} - \eta EO \tag{8}$$

Table 2
Comparison between the Nusselt number predicted by ANN against the values obtained from experiments for the test data.

Experiment No.	Input 1 (Volume fraction(%))	Input 2 (Model number)	Input 3 (Heating rate(W))	Input 4 (*Re*)	Experimental Result (*Nu*)	Network Outputs (*Nu*)	Relative Error (%)
1	1	1	50.6	400	4.1694	4.1334	0.9
2	0.5	1	50.6	1200	4.3566	4.3618	0.1
3	2	3	50.6	1200	4.6221	4.6206	0.03
4	0	2	60.7	1200	4.1239	4.1256	0.04
5	1	2	60.7	400	4.2697	4.2959	0.6
6	0.5	1	69.1	400	3.8192	3.8297	0.3
7	2	3	69.1	400	4.3769	4.3829	0.1
8	0.5	3	69.1	1200	4.4303	4.4280	0.05
							Average 0.3

where w_{new} is the adjusted weight, w_{old} is the weight before adjustment, η is the learning rate, usually chosen in the range [0 1], and E is the estimated error. Weight adjustment will be made for all connections. Errors for all train data are accumulated, and the algorithm will be run until the error falls below a predetermined value.

4. Modeling of heat transfer coefficients using ANN

The data given in Fig. 2 have been selected for ANN modeling. In the following, the details of ANN modeling have been presented.

4.1. Structure selection for ANN

To construct the neural network, a homemade MATLAB code is used. A well-trained MLP network was used to forecast the heat transfer coefficients under the condition that the inputs of the network were Reynolds number and volume fraction. The Levenberg–Marquardt algorithm was used as the training method.

Hyperbolic tangent sigmoid (tansig) and linear functions were respectively selected as the activation functions of hidden and output layers' neurons. The total number of data was 23 which 4 of them were picked out to test the network capability in predicting the heat transfer coefficients. Before train and test, the inputs and their experimental results (targets for the network) were normalized in the range of -1 and 1. So, the outputs of the network should be transferred back to their actual range to compare with the target values.

A crucial step in the neural network modeling is to select the number of hidden layers and also the number of their corresponding neurons. Here, a strategy based on the relative errors and the correlation coefficients (R^2) of the test and train data sets has been implemented to decide on the number of hidden layer and their corresponding neurons. ANNs with various structures were examined. Each network with a certain structure was run ten times.

After each run, the test data were presented to the trained network and the average of relative error per each datum and the correlation coefficients (R^2) for the test and train data sets were respectively computed. The relative error for each test datum (which were finally summed and divided by the number of test data to get the average relative error of test data in one network run) together with the R^2s (per one network run) can be evaluated as:

$$Re\,lative\ Error\,(\%) = \frac{|T - O|}{T} \times 100 \tag{9}$$

$$R_{train}^2 = \frac{\sum_{k=1}^{n_{tr}} (T_k - \overline{T}_k)(O_k - \overline{O}_k)}{\sqrt{\sum_{k=1}^{n_{tr}} (T_k - \overline{T}_k)^2 \sum_{k=1}^{n_{tr}} (O_k - \overline{O}_k)^2}} \tag{10}$$

$$R_{test}^2 = \frac{\sum_{k=1}^{n_{te}} (T_k - \overline{T}_k)(O_k - \overline{O}_k)}{\sqrt{\sum_{k=1}^{n_{te}} (T_k - \overline{T}_k)^2 \sum_{k=1}^{n_{te}} (O_k - \overline{O}_k)^2}} \tag{11}$$

where, T, O, n_{tr}, and n_{te} are the target value, the network output value, the number of train data, and the number of test data, respectively.

All aforementioned parameters were averaged for ten runs of the network. Figs. 4 and 5 demonstrate the correlation coefficients for the train and test data, respectively. It should be mentioned that notation "[m]" indicates that the network structure consists of one hidden layer including "m" neurons and "[n p]" implies that the network structure consists of two hidden layers including "n" neurons in the first and "p" neurons in the second hidden layer.

The average relative error calculated for 10 times run of each constituted network has been introduced in Fig. 6.

The above investigation on the structure of the neural network (Figs. 3-5) clarifies that a network with two hidden layers and three neurons in hidden layer 1 and two neurons in hidden layer 2 gives the best predictions of heat transfer coefficients.

4.2. Results of the selected ANN

After determination of the best structure for the neural network, the network is utilized to predict the heat transfer coefficients. Figs. 7 and 8 present the values obtained from the experiments against the predicted heat transfer coefficients values of selected network for the train and test data, respectively. Furthermore, the correlation coefficients between the target values (acquired from the experiments) and network outputs for the train and test data (${R_{train}}^2$ and ${R_{test}}^2$) are 0.9987 and 0.9997, respectively. This implies that the designed network can predict the experimental data well.

Also, for the test dataset, the relative error between the experimental results and the network outputs per each set datum has been introduced in Table 1. As seen, despite the limited available data for heat transfer coefficient; however, the average relative error is just 0.2% which reveals the high ability of trained network.

5. Nusselt number prediction using ANN

In the previous section, ANN modeling of heat transfer coefficient was performed just for heating rate of 69.1 W, in this section the modeling of Nusselt number is conducted for three values of heating rate.

5.1. Structure selection for ANN

An MLP network was trained to predict the Nusselt number while the inputs of the network were volume fraction, model number, heating rate, and Reynolds number. All the network settings except the number of hidden layers and their neurons are similar to which one used for predicting the heat transfer coefficients. Here, the total number of experimental data was 72. Among measured data, 8 data are used to test the network performance after the training procedure.

Figs. 9 and 10 reveal the correlation coefficients for the train and test data, respectively. The correlation coefficients between the target values and network outputs for the train and test datasets (${R_{train}}^2$ and ${R_{test}}^2$) are respectively 0.9970 and 0.9914.

Also, the average relative error evaluated for 10 times run of each constituted network has been presented in Fig. 11. From Figs. 9–11, it concludes that a network with two hidden layers and three neurons in each hidden layer gives the best predictions of heat transfer coefficient.

5.2. Results of the selected ANN

Figs. 12 and 13 represent the Nusselt number obtained from the experiments versus the constructed network outputs for the train and test data, respectively. In addition, Table 2 shows the results of the network against experimental results.

Figs. 12 and 13 along with Table 2 elucidate that the trained network can predict the values of Nusselt number with an average relative error of 0.3%. Such a low average relative error highlights the ability of neural network as a powerful tool to save the time and reducing the costs of study on nanofluid flow in microchannel heat sink.

6. Conclusion

Microchannel heat sinks are essential devices for cooling of electronic devices. Therefore, it makes sense for modeling and prediction of their performance, especially when an advanced working fluid like a nanofluid is used. The present study dealt with modeling of TiO_2/water nanofluid flow in a microchannel heat sink using experimental data [30]. Two different multi-layer perceptron neural networks were trained for prediction of Nusselt number and heat transfer coefficients.

For the former, the number of data was 72 while for the later the number of available data was just 23. For prediction of Nusselt number a network with two hidden layers was designed where three neurons were in each layer. The trained network for Nusselt number could predict the experimental data with an average relative error of 0.3%. To estimate the heat transfer coefficients a network with two hidden layers selected with three neurons in hidden layer 1 and two neurons in hidden layer 2. Despite the limited number of experimental data, the average relative error in prediction of heat transfer coefficients was just 0.2%. The study unveils that a well-trained neural network could be an affordable way to design of thermal systems where an experimental study may need high investment and being time-consuming.

Acknowledgement

The authors acknowledge the support provided by the "Research Chair Grant" National Science and Technology Development Agency (NSTDA), the Thailand Research Fund (TRF), the National Research University Project (NRU) and King Mongkut's University of Technology Thonburi through the "KMUTT 55th Anniversary Commemorative Fund".

References

[1] R. Saidur, K.Y. Leong, H.A. Mohammad, A review on applications and challenges of nanofluids, Renew. Sust. Energy Rev. 15 (3) (2011) 1646–1668.
[2] O. Mahian, A. Kianifar, S.A. Kalogirou, I. Pop, S. Wongwises, A review of the applications of nanofluids in solar energy, Int. J. Heat Mass Transf. 57 (2) (2013) 582–594.
[3] W. Daungthongsuk, S. Wongwises, A critical review of convective heat transfer of nanofluids, Renew. Sust. Energy Rev. 11 (5) (2007) 797–817.
[4] V. Trisaksri, S. Wongwises, Critical review of heat transfer characteristics of nanofluids, Renew. Sust. Energ. Rev. 11 (3) (2007) 512–523.
[5] S.Z. Heris, M.B. Pour, O. Mahian, S. Wongwises, A comparative experimental study on the natural convection heat transfer of different metal oxide nanopowders suspended in turbine oil inside an inclined cavity, Int. J. Heat Mass Transf. 73 (2014) 231–238.
[6] A. Kasaeian, R.D. Azarian, O. Mahian, L. Kolsi, A.J. Chamkha, S. Wongwises, I. Pop, Nanofluid flow and heat transfer in porous media: a review of the latest developments, Int. J. Heat Mass Transf. 107 (2017) 778–791.
[7] J. Cai, X. Hu, B. Xiao, Y. Zhou, W. Wei, Recent developments on fractal-based approaches to nanofluids and nanoparticle aggregation, Int. J. Heat Mass Transf. 105 (2017) 623–637.
[8] M.H. Esfe, S. Saedodin, S. Wongwises, D. Toghraie, An experimental study on the effect of diameter on thermal conductivity and dynamic viscosity of Fe/water nanofluids, J. Therm. Anal. Calorim. 119 (2015) 1817–1824.
[9] O. Mahian, A. Kianifar, S.Z. Heris, D. Wen, A.Z. Sahin, S. Wongwises, Nanofluids effects on the evaporation rate in a solar still equipped with a heat exchanger, Nano Energy 36 (2017) 134–155.
[10] S.S. Meibodi, A. Kianifar, H. Niazmand, O. Mahian, S. Wongwises, Experimental investigation on the thermal efficiency and performance characteristics of a flat plate solar collector using SiO_2/EG–water nanofluids, Int. Commun. Heat Mass Transf. 65 (2017) 71–75.
[11] A.K. Santra, N. Chakraborty, S. Sen, Prediction of heat transfer due to presence of copper–water nanofluid using resilient-propagation neural network, Int. J. Therm. Sci. 48 (7) (2009) 1311–1318.
[12] M. Hojjat, S.Gh. Etemad, R. Bagheri, J. Thibault, Thermal conductivity of non-Newtonian nanofluids: experimental data and modeling using neural network, Int. J. Heat Mass Transf. 54 (2011) 1017–1023.
[13] M. Balcilar, A.S. Dalkilic, A. Suriyawong, T. Yiamsawas, S. Wongwises, Investigation of pool boiling of nanofluids using artificial neural networks and correlation development techniques, Int. Commun. Heat Mass Transf. 39 (3) (2012) 424–431.
[14] F. Yousefi, H. Karimi, M.M. Papari, Modeling viscosity of nanofluids using diffusional neural networks, J. Mol. Liq. 175 (2012) 85–90.
[15] M.H. Esfe, S. Saedodin, M. Bahiraei, D. Toghraie, O. Mahian, S. Wongwises, Thermal conductivity modeling of MgO/EG nanofluids using experimental data and artificial neural network, J. Therm. Anal. Calorim. 118 (2014) 287–294.
[16] M. Bahiraei, P.R. Mashaei, Using nanofluid as a smart suspension in cooling channels with discrete heat sources, J. Therm. Anal. Calorim. 119 (2015) 2079–2091.
[17] M.H. Esfe, A. Naderi, M. Akbari, M. Afrand, A. Karimipour, Evaluation of thermal conductivity of COOH-functionalized MWCNTs/water via temperature and solid volume fraction by using experimental data and ANN methods, J. Therm. Anal. Calorim. 121 (2015) 1273–1278.
[18] M. Afrand, K.Na. Najafabadi, N. Sina, M.R. Safaei, A.Sh. Kherbeet, S. Wongwises, M. Dahari, Prediction of dynamic viscosity of a hybrid nano-lubricant by an optimal artificial neural network, Int. Commun. Heat Mass Transf. 76 (2016) 209–214.
[19] A. Abdollahi, M. Shams, Optimization of heat transfer enhancement of nanofluid in a channel with winglet vortex generator, Appl. Therm. Eng. 91 (2015) 1116–1126.
[20] M. Ziaei-Rad, M. Saeedan, E. Afshari, Simulation and prediction of MHD dissipative nanofluid flow on a permeable stretching surface using artificial neural network, Appl. Therm. Eng. 99 (2016) 373–382.
[21] H. Kalani, M. Sardarabadi, M. Passandideh-Fard, Using artificial neural network models and particle swarm optimization for manner prediction of a photovoltaic thermal nanofluid based collector, Appl. Therm. Eng. 113 (2017) 1170–1177.
[22] A. Barati-Harooni, A. Najafi-Marghmaleki, An accurate RBF-NN model for estimation of viscosity of nanofluids, J. Mol. Liq. 224 (2016) 580–588.
[23] A. Aminian, Predicting the effective thermal conductivity of nanofluids for intensification of heat transfer using artificial neural network, Powder Technol. 301 (2016) 288–309.
[24] M. Afranda, A. Ahmadi Nadooshan, M. Hassani, H. Yarmand, M. Dahari, Predicting the viscosity of multi-walled carbon nanotubes/water nanofluid by developing an optimal artificial neural network based on experimental data, Int. Commun. Heat Mass Transf. 77 (2016) 49–53.
[25] M. Saeedan, A.R. Solaimany Nazar, Y. Abbasi, R. Karimi, CFD investigation and neutral network modeling of heat transfer and pressure drop of nanofluids in double pipe helically baffled heat exchanger with a 3-D fined tube, Appl. Therm. Eng. 100 (2016) 721–729.
[26] M. Vafaei, M. Afrand, N. Sina, R. Kalbasi, F. Sourani, H. Teimouri, Evaluation of thermal conductivity of MgO-MWCNTs/EG hybrid nanofluids based on experimental data by selecting optimal artificial neural networks, Physica E Low Dimens. Syst. Nanostruct. 85 (2017) 90–96.
[27] M.H. Esfe, K. Motahari, E. Sanatizadeh, M. Afrand, H. Rostamian, M.R. Hassani Ahangar, Estimation of thermal conductivity of CNTs-water in low temperature by artificial neural network and correlation, Int. Commun. Heat Mass Transf. 76 (2016) 376–381.
[28] M. Afrand, M. Hemmat Esfe, E. Abedini, H. Teimouri, Predicting the effects of magnesium oxide nanoparticles and temperature on the thermal conductivity of water using artificial neural network and experimental data, Physica E Low Dimens. Syst. Nanostruct. 87 (2017) 242–247.
[29] H. Shokouhmand, M. Ghazvini, J. Shabanian, Analysis of Microchannel Heat Sink Performance Using Nanofluids in Turbulent and Laminar Flow Regimes and Its Simulation Using Artificial Neural Network, Tenth International Conference on Computer Modeling and Simulation (Uksim 2008), (2008), pp. 623–628.
[30] P. Nitiapiruk, O. Mahian, A.S. Dalkilic, S. Wongwises, Performance characteristics of a microchannel heat sink using TiO_2/water nanofluid and different thermophysical models, Int. Commun. Heat Mass Transf. 47 (2013) 98–104.
[31] O. Mahian, A. Kianifar, C. Kleinstreuer, M.A. Al-Nimr, I. Pop, A.Z. Sahin, S. Wongwises, A review of entropy generation in nanofluid flow, Int. J. Heat Mass Transf. 65 (2013) 514–532.
[32] W. Yu, S.U.S. Choi, The role of interfacial layers in the enhanced thermal conductivity of nanofluids: a renovated Maxwell model, J. Nanopart. Res. 5 (2003) 167–171.
[33] W. Duangthongsuk, S. Wongwises, Measurement of temperature-dependent thermal conductivity and viscosity of TiO_2 water nanofluids, Exp. Thermal Fluid Sci. 33 (2009) 706–714.
[34] G.E. Cook, R.J. Barnett, K. Andersen, A.M. Strauss, Weld modeling and control using artificial neural networks, IEEE Trans. Ind. Appl. 31 (6) (1995).
[35] D.E. Rumelhart, J.L. Mcclelland, Parallel Distributed Processing: Explorations in the Microstructure of Cognition, 1 MIT Press, 1986.